Inorg. Chem. **2008**, *47*, 10798−10800

Photoluminescent Mn_4 Single-Molecule Magnet

Christopher C. Beedle,[†] Casey J. Stephenson,[†] Katie J. Heroux,[†] Wolfgang Wernsdorfer,[‡] and David N. Hendrickson*[,†]

Department of Chemistry and Biochemistry, University of California at San Diego, La Jolla, California 92093-0358, and Institut Néel, CNRS, BP166, Grenoble Cedex 9, France

Received August 5, 2008

The synthesis of $[Mn_4(anca)_4(Hmdea)_2(mdea)_2]\cdot 2CHCl_3$ (**1**) is reported along with room temperature fluorescence, UV−vis, and NMR spectra. Direct current magnetization versus field data reveal a $S = 8$ ground state. Quantized steps in temperature- and field-dependent magnetization versus field hysteresis loops confirm single-molecule magnet behavior.

There is currently much interest in polynuclear transition-metal complexes that function as single-molecule magnets (SMMs).[1] The large spin ground state (S) and appreciable magnetoanisotropy (D) exhibited by these complexes lead to a barrier to the reversal of magnetization ($|D|S_z^2$). Most notably, these complexes have been shown to exhibit interesting physical phenomena such as quantum tunneling of magnetization (QTM), spin-parity effects, spin−spin cross-relaxation, and coherence effects.[2a−f]

In recent years, progress[4a,b] has been made in understanding SMMs employing techniques such as single-crystal high-frequency electron paramagnetic resonance and the micro-SQUID array.[3] Although these techniques are paramount to the study of SMMs at the single-crystal level, there is intense interest in performing studies at the single-molecule level. Though application to the study of SMMs has not been realized, single-molecule spectroscopy[5a,b] has yielded a great deal of insight into the electronic and vibronic structures of photoluminescent organics isolated in a solid matrix. Recently, efforts have been made to study SMMs at the single-molecule level by placing them on surfaces to examine their conductive properties as they relate to molecular electronics.[6a−e] However, it can often be difficult to determine the exact position or dispersion of species deposited on surfaces (e.g., one, two, or more molecules or clusters of molecules may be present). When SMMs are employed with photoluminescent properties, it may be possible to precisely ascertain the positions and concentration of molecules on surfaces. Furthermore, if the photoexcited states of photoluminescent ligands are coupled directly to the magnetic moment of a SMM (below their blocking temperature, T_B), this may provide a new tool for studying the fundamental quantum behavior exhibited by SMMs on a $10^{-9}-10^{-12}$ s time scale.

Herein we report the synthesis and physical properties of $[Mn_4(anca)_4(Hmdea)_2(mdea)_2]\cdot 2CHCl_3$ (**1**;[7] Figure 1), where $anca^-$ is the anion of 9-anthracenecarboxylic acid and $Hmdea^-$ and $mdea^{2-}$ are the monoanion and dianion of *N*-methyldiethanolamine, respectively.

Complex **1** crystallizes in the triclinic space group $P\bar{1}$ with four symmetry-independent halves of the molecule and four chloroform solvate molecules in the asymmetric unit. Each molecule consists of an oxo-bridged $[Mn^{II}_2Mn^{III}_2O_6]^{4+}$ core resembling two face-sharing cubanes missing opposite

* To whom correspondence should be addressed. E-mail: dhendrickson@ucsd.edu. Fax: +858-534-5383.
† University of California, San Diego.
‡ Institut Néel.

(1) Aubin, S. M. J.; Wemple, M. W.; Adams, D. M.; Tsai, H. L.; Christou, G.; Hendrickson, D. N. *J. Am. Chem. Soc.* **1996**, *118* (33), 7746–7754.
(2) (a) Sessoli, R.; Gatteschi, D.; Caneschi, A.; Novak, M. A. *Nature* **1993**, *365* (6442), 141–143. (b) Sessoli, R.; Tsai, H. L.; Schake, A. R.; Wang, S. Y.; Vincent, J. B.; Folting, K.; Gatteschi, D.; Christou, G.; Hendrickson, D. N. *J. Am. Chem. Soc.* **1993**, *115* (5), 1804–1816. (c) Hill, S.; Edwards, R. S.; Aliaga-Alcalde, N.; Christou, G. *Science* **2003**, *302* (5647), 1015–1018. (d) Wernsdorfer, W.; Bhaduri, S.; Boskovic, C.; Christou, G.; Hendrickson, D. N. *Phys. Rev. B* **2002**, *65* (18), 180403. (e) Wernsdorfer, W.; Bhaduri, S.; Tiron, R.; Hendrickson, D. N.; Christou, G. *Phys. Rev. Lett.* **2002**, *89* (19), 197201. (f) Christou, G.; Gatteschi, D.; Hendrickson, D. N.; Sessoli, R. *MRS Bull.* **2000**, *25* (11), 66–71.
(3) Wernsdorfer, W. *Adv. Chem. Phys.* **2001**, *118*, 99–190.
(4) (a) Wernsdorfer, W.; Allaga-Alcalde, N.; Hendrickson, D. N.; Christou, G. *Nature* **2002**, *416* (6879), 406–409. (b) Wernsdorfer, W.; Aliaga-Alcalde, N.; Tiron, R.; Hendrickson, D. N.; Christou, G. *J. Magn. Magn. Mater.* **2004**, *272*−*276*, 1037–1041.
(5) (a) Kulzer, F.; Orrit, M. *Annu. Rev. Phys. Chem.* **2004**, *55* (1), 585–611. (b) Moerner, W. E.; Kador, L. *Phys. Rev. Lett.* **1989**, *62* (21), 2535.
(6) (a) Jo, M. H.; Grose, J. E.; Baheti, K.; Deshmukh, M. M.; Sokol, J. J.; Rumberger, E. M.; Hendrickson, D. N.; Long, J. R.; Park, H.; Ralph, D. C. *Nano Lett.* **2006**, *6* (9), 2014–2020. (b) Ni, C.; Shah, S.; Hendrickson, D.; Bandaru, P. R. *Appl. Phys. Lett.* **2006**, *89* (21), 212104. (c) Bogani, L.; Wernsdorfer, W. *Nat. Mater.* **2008**, *7*, 179–186. (d) Coronado, E.; Martí-Gastaldo, C.; Tatay, S. *Appl. Surf. Sci.* **2007**, *254*, 225–235. (e) Abdi, A. N.; Bucher, J. P.; Rabu, P.; Toulemonde, O.; Drillon, M.; Gerbier, P. *J. Appl. Phys.* **2004**, *95*, 7345–7347.
(7) Synthesis of complex **1**: $MnCl_2\cdot 4H_2O$ (200 mg, 1.01 mmol) and 9-anthracenecarboxylic acid (222 mg, 1.00 mmol) were dissolved in 20 mL of a 2:1 solution of $CHCl_3$ and MeOH, affording a pale-yellow solution. To the resulting solution was added dropwise *N*-methyldiethanolamine (241 mg, 2.02 mmol). The dark-brown solution was stirred for 30 min and subsequently gravity filtered and layered with acetonitrile, yielding dark-brown plates of X-ray quality after 1 week.

10.1021/ic801485k CCC: $40.75

Published on Web 10/24/2008

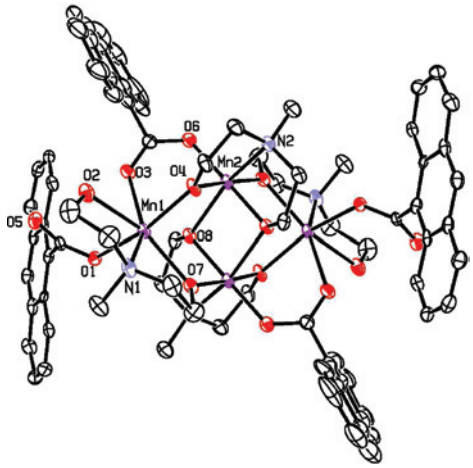

Figure 1. ORTEP drawing of **1** with thermal ellipsoids at 30% probability. Hydrogen atoms have been removed for clarity.

vertices (the shared face consists of Mn2−O8 and their inversion symmetry equivalents). The divalent Mn1 ions are arranged in a distorted pentagonal-bipyramidal geometry, where three of the coordination positions in the pentagonal plane are occupied by an $Hmdea^-$ ligand. The apical positions are occupied by a carboxylate O1 atom of a pendant monodentate $anca^-$ ligand and an alkoxy O4 atom that also serves as a $Mn1^{II}$−O4−$Mn2^{III}$ bridge. A tridentate $Hmdea^-$ ligand bridges between $Mn1^{II}$ and $Mn2^{III}$ atoms. The final two coordination positions are occupied by a $anca^-$ oxo and a $Mn1^{II}$−O−$Mn2^{III}$ bridging O8 alkoxy arm from one of the two dianionic $mdea^{2-}$ ligands. The trivalent Mn2 ions are arranged in a tetragonally distorted octahedral environment capped by a tridentate $mdea^{2-}$ ligand. Oxidation states were determined by the presence of Jahn−Teller (JT) elongations and bond valence sum (BVS) calculations (Table S1 in the Supporting Information). The single-ion tetragonally elongated JT axes for the two Mn^{III} ions of each molecule are collinear and lie along the N2−Mn2−O8 bonds. However, the JT projections of all of the molecules within the unit cell are not mutually collinear because of the presence of four symmetry-independent species.

To obtain the spin ground state and gauge Hamiltonian parameters such as the zero-field-splitting parameter D, rhombic term E, and Zeeman interactions, reduced magnetization ($M/N\beta$ vs H/T) data were collected for **1** (Figure S1 in the Supporting Information) between 1.8 and 4.0 K with applied fields of 0.1−5 T. Experimental data were least-squares fit to eq 1, where $\hat{S}_i$ is the spin projection operator, g is the Landé g factor, μ_B is the Bohr magneton, and B is the applied magnetic field. The best fit (S1) yielded parameters of $S = 8$, $g = 1.95$, $D = -0.28$ cm^{-1}, and $E = 0.08$ cm^{-1}.

$$H = D\hat{S}_z^2 + E(\hat{S}_x^2 - \hat{S}_y^2) + g\mu_B\hat{S}\cdot B \qquad (1)$$

To determine if complex **1** is a SMM, oriented single-crystal magnetization versus field hysteresis experiments were performed. Because the projections of the easy axes of the four symmetry-independent molecules are not collinear, the angle of the applied field relative to the easy axis of each molecule was calculated to be 45°. Steps in the

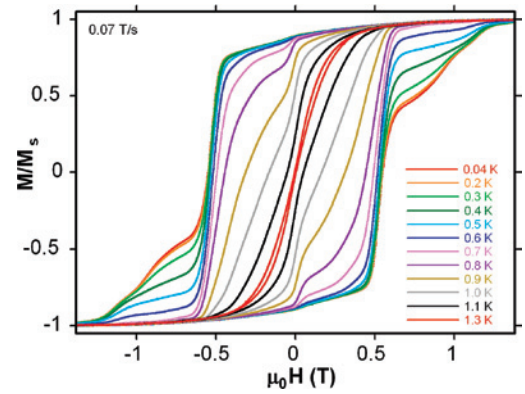

Figure 2. Plot of temperature-dependent magnetization versus field hysteresis loops for complex **1**.

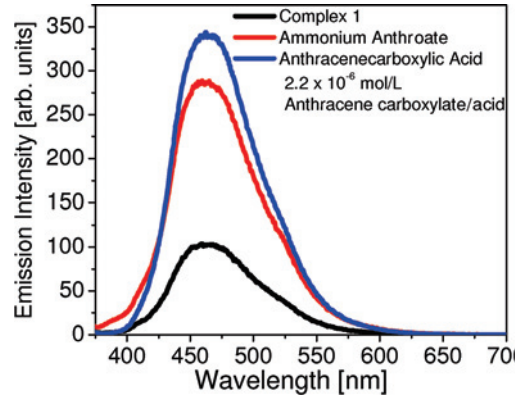

Figure 3. Room temperature fluorescence emission spectra for 9-anthracenecarboxylic acid (A, blue), complex **1** (black), and ammonium 9-anthroate (B, red) collected at 10^{-6} M in dichloromethane.

exhibited temperature-dependent (Figure 2) and field-sweep-rate-dependent (S2) hysteresis loops, indicative of QTM, confirm that complex **1** is a SMM. Detailed analysis of magnetization hysteresis data and magnetic susceptibility data will be presented in a future publication.

Room temperature fluorescence emission spectra for Hanca, NH_4-anca, and complex **1** are given in Figure 3. Fluorescence data were collected in CD_2Cl_2 with fluorophore concentrations of 10^{-6} M. The emission spectrum of complex **1** exhibits the same line shape and peak position (460 nm) as those of Hanca and NH_4-anca, as previously documented.[8] A comparison of the three spectra in Figure 3 reveals significant quenching of the emission intensity for **1** due to paramagnetic effects. Figure 4 illustrates room temperature UV−vis data for Hanca, NH_4-anca, and complex **1** in CD_2Cl_2 with fluorophore concentrations of 10^{-5} M. Discernible peak position shifts (4 nm) to lower energy are clearly evident for absorption bands II−V, and band I is only evident in the absorption spectrum of **1**. Furthermore, the peak line shapes (bands III−V) for **1** are sharper than the corresponding absorption bands for Hanca and NH_4-anca. A comparison of calculated molar extinction coefficients for Hanca, NH_4-anca, and complex **1** from UV−vis molar absorbance data reveals a 2-fold extinction coefficient increase in complex **1**

(8) Abdel-Mottaleb, M. S. A.; Galal, H. R.; Dessouky, A. F. M.; El-Naggar, M.; Mekkawi, D.; Ali, S. S.; Attya, G. M. *Int. J. Photoenergy* 2 **2000**, 47–53.

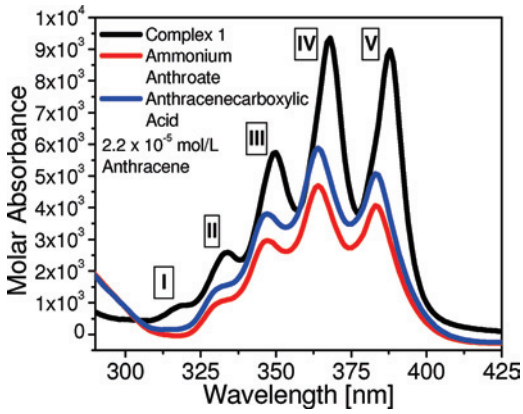

Figure 4. Room temperature UV−vis spectra for 9-anthracenecarboxylic acid (A, blue), complex **1** (black), and ammonium 9-anthroate (B, red) collected at 10^{-5} M in dichloromethane, plotted as molar absorbance versus wavelength.

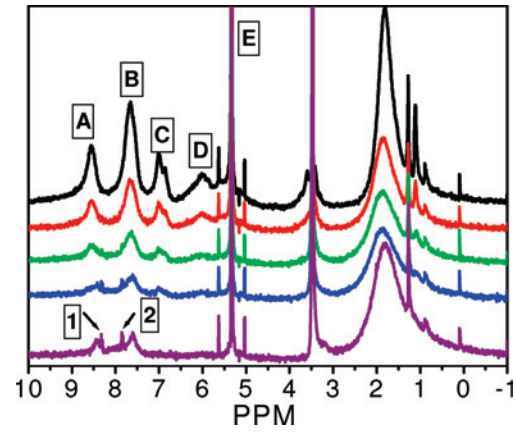

Figure 5. NMR spectra collected by successive additions of 0.08 mL of NH_4-anca in CD_2Cl_2 into complex **1** (top, black trace). Peak E is the solvent reference peak.

relative to Hanca and NH_4-anca, indicating that the electronic environment of the anthacenecarboxylates is significantly modulated when coordinated to Mn ions. However, it is important to ascertain whether spectral changes can be interpreted as arising from energy shifts in $\pi-\pi^*$ transitions originating from bound anca$^-$ ligands or whether spectral peak shifts are a result of free anca$^-$ anions or exchanging anca$^-$ anions interacting with paramagnetic Mn ions in solution. In order to address whether complex **1** is intact in solution, detailed UV−vis and NMR experiments were performed.

UV−vis spectral data from the addition of 0.25 mL aliquots of 10^{-5} M NH_4-anca in CD_2Cl_2 to a 10^{-5} M (by fluorophore) solution of complex **1** are presented in Figure S3 in the Supporting Information. It is evident from Figure S3 that sequential additions of anca$^-$ and a subsequent decrease in the complex **1** concentration lead to a shift in the corresponding peak positions II−V and broadening of spectral line shapes. Furthermore, the systematic disappearance of peak I is in agreement with the UV−vis spectra in Figure 4 of complex **1** and NH_4-anca, respectively. This strongly indicates that the line shape and intensity of the UV−vis spectrum of complex **1** (Figure 4) are not due to free anions in solution.

Peak broadening in NMR experiments arises from a number of factors including ligand-exchange and paramagnetic effects. The NMR spectrum of complex **1** in CD_2Cl_2 (top trace, black) is presented in Figure 5. To determine if complex **1** is intact in solution, NH_4-anca in CD_2Cl_2 was sequentially added in 0.08 mL aliquots (red, green, blue, and purple traces, Figure 5) and the evolution of the proton signals was monitored. As the concentration of the anion was increased, proton signals A−D systematically disappeared (peaks A−C are the proton signals assigned to the conjugated anthacene ring protons).[9] At concentrations approaching 90% anion (bottom trace, purple, Figure 5), the peaks labeled 1 and 2 begin to emerge and are consistent with the proton signals seen in the NMR of pure NH_4-anca in CD_2Cl_2 (Figure S4 in the Supporting Information). Thus, the spectral data in Figure 5 clearly support that the free anion is not a significant species in solution. Rather, NMR spectral features for complex **1** are dominated by anca$^-$ ligands bound to the Mn_4 complex. This is further substantiated by the fact that if complex **1** in CD_2Cl_2 is allowed to evaporate, the only product recovered is the original complex. Additionally, there is little stabilization in dichloromethane (aprotic) for the free anion.

SMMs with emissive ligands are attractive media for two important reasons. First, above the blocking temperature (T_B), the magnetic dipole moment of a SMM is rapidly changing between "spin-up" and "spin-down" orientations. However, when the temperature of the SMM is lowered below T_B, the molecular dipole moments become fixed in orientation (spontaneous magnetization). Thus, the fluorescent lifetimes of the emissive ligands may be dramatically affected. Second, the presence of emissive ligands could prove valuable in the detection of single molecules, which is an issue of vital importance in the field of molecular electronics.

In conclusion, a new $[Mn^{II}_2Mn^{III}_2]$ dicubane SMM with photoluminescent properties has been synthesized. The complex possesses significant axial magnetoanisotropy and a $S = 8$ spin ground state. Furthermore, we have synthesized a series of related Mn_4 SMMs that differ in their peripheral photoluminescent ligands and R group of their tripodal diethanolamine ligands (H_2Rdea). In this family of SMMs, subtle changes in the luminescent lifetimes and steric considerations may have a dramatic affect on their magnetic properties. Efforts are currently underway to perform simultaneous fluorescent and magnetization measurements below their blocking temperatures ($T_B = 0.9$ K for $\tau = 100$ s for **1**), and the results will be published at a later date.

Acknowledgment. This work was supported by the National Science Foundation.

Supporting Information Available: X-ray crystallography (CCDC 697092), BVS analysis, ^{1}H NMR, and supplemental magnetization data. This material is available free of charge via the Internet at http://pubs.acs.org.

IC801485K

(9) Spectral Database for Organic Compounds. SDBS No. 11061.